Available online www.unicrossjournals.com

UNICROSS JOURNAL OF SCIENCE AND TECHNOLOGY, UJOST

RESEARCH ARTICLE VOL. 1(2) SEPTEMBER, 2022 ISSN:2814-2233

Date Accepted: 31st August, 2022 Pages 91 - 108

ON DETERMINISM, WELL-POSEDNESS AND THE APPLICATION OF CAUCHY-LIPSCHITZ CONDITIONS FOR A HYPO-HYPER COVID-19 EPIDEMIC MODEL

[1*]**Bassey Echeng Bassey**,[2]**Igwe O. Ewona**

[1]Department of Mathematics, University of Cross River State – (Unicross),

[2]Department of Physics, University of Cross River State – (Unicross),

Calabar, Nigeria,

[*]Corresponding author email:awaserex@ymail.com

Abstract

In spite of avalanche preventive and treatment measures for the control of the dreaded COVID-19 disease, scientists and the health sectors are yet to ascribe an outright medical prescription for the aforementioned viral load. A situation that is further aggravated by the continuous emergence of varying strings of the viral load. In this present study, tinkering on formulating coherent control measure in Nigeria, with the incorporation of a triple-bilinear control functions, we present a theoretical prediction model that accounts for the determinisms of globally feasible COVID-19 mathematical model under a hypo-hyper infectious environs. The goal of the study is to investigate the viability and well-posedness of the derived model. Under an expanded 10-Dimensional deterministic sub-population, the study explored classical fundamental theory of differential equations with the incorporation of Cauchy-Lipschitz conditions. The results of numerical simulations, does not only affirmed the non-negativity model state-space but remarkably, established the model of well-posedness.

Keywords: Triple-bilinear control, hypo-hyper-infection, super-spreader, Cauchy-Lipschitz-condition, well-posedness

1. Introduction

In history of mankind in relation to infectious diseases, the global world was and is still been subjected to an unprecedented death toll, loss of manpower and economy degradation by the ravaging infectious disease called Coronavirus 2019 or COVID-19. Perturbingly, is the fact that the history of COVID-19 in terms of its origin, transmission mode and controls will for a long period remain sacrosanct in the scientific world, following it emergence in late December, 2019, in the city of Wuhan, China [1,2,3].

Zoonotic have confirmed that the transmission capability of the virus is exponential in nature following it

asymptomatic incubation period of $2-14$ days, which is often buttress by it less clinical manifestation but highly infectious [4,5,6,7]. The spread of the virus have been adjudged to cut across all human-race, sexes having the elderly age ≥ 65 years becoming more vulnerable, [8,9,10]. The main reservoir of COVID-19 among other notable outlets is the environment (space), which when in contact with human, lead to environment-to-human (hypo-infectious) transmit; and the human-to-human (hyper-infectious) transmit [11,12,13].

Mathematical modeling among other approaches, have been a method through which scientific investigations are being conducted in understanding both the transmission and control mechanisms of the virus. For instance, a number of models have been formulated that study either of the aforementioned transmission modes. The study [11], using under environment-to-human mode, investigated the transmissibility of novel COVID-19 using bats-Host-reservoir-people transmission approach. Considering multiple preventive and treatment measures, a dual-bilinear controls was used to study the interactions between host viral loads and varying subpopulations under human-to-human transmission mode [4]. In this study, the model explores deterministic approach leaving a very high significant results. For more mathematical models on COVID-19, see for examples [14,15,16,17,18,19]. Notably, further reviews have shown that methodological combinations for triple-bilinear control functions in presence of hypo-hyper transmission modes have not been the desired attention within the ambits of the global world.

Therefore, accounting for the aforementioned limitations, this present proposed model in considering a triple-bilinear controls on an expanded 10-Dimensional deterministic model, concurrently tinker towards accounting for the methodological combinations of hypo-hyper transmission modes. More so, the study seeks not only to importantly, verify the well-posedness of the anticipated complex proposed model but also, investigate the positivity of the ascribed state-space of the model and the uniqueness of solution using the Lipschitz condition. In particular, Lipschitz condition is defined as: a function $f:[a,b]\to\Re$ is said to satisfy the Lipschitz condition if there is a constant M such that $|f(x)-f(x')|\leq M|x-x'| \ \forall \ x,x'\in[a,b]$,where M is the Lipschitz constant.

Knowledgeably, while section 1 explicitly highlighted the introductory part, section 2, treats the materials and methods, defined by the study problem statement and derivation proposed model. Section 3 is devoted to the determination of model mathematical properties. The numerical illustrations and results analysis are presented in section 4 and finally, the discussion as well as conclusion of study forms the pivot of section 5. Most remarkably, the verification of the present formulation is particularly for a complex model of its magnitude, a most vital step worthy of investigation.

2. Material and methods

In this present proposal, which is conceived as a prerequisite to a forthcoming research on the application of triple-bilinear control functions for COVID-19 treatment dynamics,

we seek to present theoretical predictions that account for the determinism and the well-posedness of a hypo-hyper COVID-19 infection model. The material here shall be constituted by the interactions of aerosol viral load with 10-Dimenssional deterministic dynamic population to be investigated using designated triple-bilinear control functions in the form: a bilinear non-pharmaceutical (face-masking and social distancing), bilinear pharmacotherapies (hydroxylchloroquine - HCQ and azithromycin – AZT) and bilinear immunity controls (adaptive immune response and **BNT162b2** – vaccine). Theoretical analysis shall explore classical fundamental theory of differential equations with the incorporation Cauchy-Lipschitz conditions. Remarkably, we intend to explore the material and methods for this present investigation as a function of study problem statement arising from study motivational model and the derivation of study mathematical equations.

2.1 Problem statement of proposed study

For this investigation, we present a succinct review of two compactible motivating models. For instance, a COVID-19 transmission model, which studied case of COVID-19 infection in Wuhan, China, early 2020, was conducted [1]. The model was formulated and studied with the aim of giving an insight to the transmission mode and the consequential behavioral attitude upon becoming aware of infection status. Of note, the study was devoid of any control functions. Following the significant results thereof, the model was extended and redefined with incorporation of screening method and studied under dual-bilinear control functions (bilinear non-pharmaceutical – face-masking and social distancing and bilinear pharmacotherapy – hydroxylchloroquine, HCQ and azithromycin, AZT), [4]. The results were emphatically significant and served as a leeway to future and related studies by the scientific communities.

None-the-less, these two models were not without its lapses, which include the fact that both studies were devoid of the role of available vaccines. More so, the dual role of adaptive immune effectors as well as immunity delay lag were not given the desired attention. Therefore, in attempt to incorporate the aforementioned lapses, the present study seeks to present an expanded 10-Dimensional deterministic dynamic mathematical model that incorporate the aforementioned limitation and sought to give an insight to both the transmission and enhanced treatment dynamics of the deadly disease.

2.2 Derived equations for proposed model

Following the aforementioned limitations, the present model is propose is an improved expanded 10-Dimensioanl deterministic mathematical dynamic model, constituted by a set of susceptible $S_p(t)$, the exposed class $X_p(t)$, the unaware asymptomatic infectious population $A_u(t)$, subpopulation of COVID-19 aware infectives $I_a(t)$, isolated infectious subpopulation $I_s(t)$, proportion of super-spreaders $S_s(t)$, proportion of hospitalized infectives $H_i(t)$, recovered population $R_p(t)$, the immune effectors $E_i(t)$ and $C_v(t)$ representing the concentration of infectious coronavirus. Thus, this proposed model is bounded by the following assumption in addition to those of its motivating models:

Assumption 1:

i. All state-space are all non-negative i.e. $N_i > 0$.

ii. All the state-space are bounded i.e. $0 \le N_i(t) \le \infty$

iii. Only severely infectious die due to virus i.e. $\alpha_{i=1,..,5} \ge 0$.

Moreso, if the control functions known as triple bilinear include: bilinear non-pharmaceuticals (face-masking and social distancing), bilinear pharmacotherapies (hydroxylchloroquine - HCQ and azithromycin – AZT) and bilinear immunity controls (adaptive immune response and **BNT162b2** – vaccine), then for the population with volume measure in $cells/ml^3$, the differential epidemiological dynamic equations for the present study is derived as:

$$\frac{dS_p}{dt} = b_p + m_1 E_i \sigma_1 X_p + \sigma_2 R_p - \beta_i(\hat{N}) S_p - (\mu + v_1) S_p,$$

$$\frac{dX_p}{dt} = \beta_i(\hat{N}) S_p + m_2 E_i \sigma_3 A_u - (1-u_1)\lambda X_p - (\mu + m_1 \sigma_1 E_i) X_p,$$

$$\frac{dA_u}{dt} = (1-u_1)\lambda X_p - [(1-u_2)k\theta + (1-a_1)(1-a_2)\varphi_1 + \varphi_2] e^{-\omega_1 \alpha_1} A_u - (\mu + m_2 E_i \sigma_3) A_u,$$

$$\frac{dI_a}{dt} = (1-u_2)k\theta e^{-\omega_1 \alpha_1} A_u - [(1-a_1)(1-a_2)\rho_2 + a_1 \tau_1 \rho_1 + (1-\rho_1-\rho_2)] I_a - \alpha_2 I_a,$$

$$\frac{dI_s}{dt} = a_1 \tau_1 \rho_1 I_a + a_1 \tau_2 \gamma_s S_s - [(1-a_1)(1-a_2)\delta_h] I_s - (\alpha_4 + v_2 \eta_2) I_s,$$

$$\frac{dS_s}{dt} = \varphi_2 e^{-\omega_1 \alpha_1} A_u + (1-\rho_1-\rho_2) I_a - a_1 \tau_2 \gamma_s S_s - [(1-\rho_1-\rho_2)\varphi_2] e^{-\omega_2 \alpha_1} S_s - (\alpha_5 + \eta_3) S_s,$$

$$\frac{dH_i}{dt} = \begin{cases} (1-a_1)(1-a_2)\varphi_1 e^{-\omega_1 \alpha_1} A_u + (1-a_1)(1-a_2)[\rho_2 I_a + \delta_h I_s] \\ -[(1-a_1)(1-a_2)[\varphi_1 + \rho_2 + \delta_h]] e^{-\omega_2 \alpha_1} H_i - (\alpha_3 + \eta_1) H_i \end{cases}, \quad (1)$$

$$\frac{dC_v}{dt} = s\left(1 - \frac{C_v}{Q}\right) C_v + (1-\rho_1-\rho_2)\varphi_2 e^{-\omega_2 \alpha_1} S_s + [(1-a_1)(1-a_2)[\varphi_1 + \rho_2 + \delta_h]] e^{-\omega_2 \alpha_1} H_i - \mu_v C_v,$$

$$\frac{dR_p}{dt} = \eta_1 H_i + v_2 \eta_2 I_s + \eta_3 S_s + v_1 S_p - (\mu + \sigma_2) R_p,$$

$$\frac{dE_i}{dt} = \zeta_E + \frac{b_E (S_s + H_i)}{(S_s + H_i) + C_b} E_i - \frac{d_E (S_s + H_i)}{(S_s + H_i) + C_d} E_i - \mu_E E_i,$$

with initial conditions $S_p(t_0) > 0, \quad X_p(t_0) > 0, \quad A_u(t_0) > 0, \quad I_a(t_0) > 0, \quad I_s(t_0) > 0, \quad S_s(t_0) > 0, \quad H_i(t_0) > 0, \quad R_p(t_0) > 0$, $C_v(t_0) > 0$, $E_i(t_0) > 0$ for all $t = t_0$ and having system mass action $\beta_i(\hat{N}_i)$ defined by

$$\beta_i(\hat{N}) = (1-u_1-u_2)\left[\frac{\phi C_v}{Q + C_V}\left(\sum_{i=1}^{5} \beta_i c_i(\hat{N}_i)\right)\right], i = 1,....,5, \quad (2)$$

where $\hat{N}_i = (X_p + A_u + I_a + S_s + H_i)$ .Of note, system (1) represent an expanded environmental-to-human (hypo infectious) and human-to-human (hyper-infectious) untreated COVID-19 dynamic model, provided control functions c_f is such that $c_f \equiv (u_i, a_i, m_i, v_i) = 0$, $i = 1,2$ for all $\beta_i(\hat{N}) > 0, i = 1,...,5$.

Therefore, accounting for assumption 1 and system (1), we represent in fig. 1, below, the graphical image of derive model

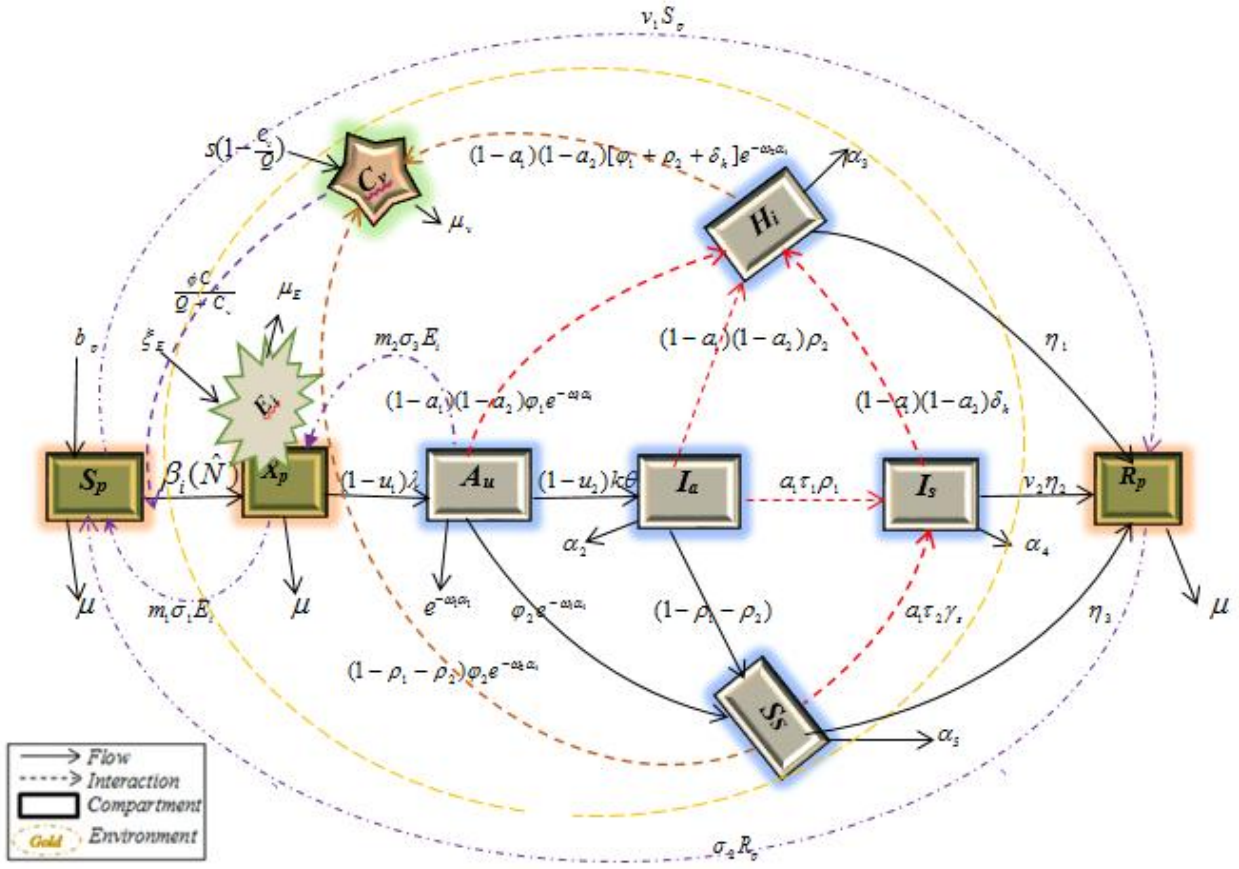

Fig. 1. Graphic image ofCOVID-19 infection dynamic under multi-therapies and vaccination control functions

The detail description for system (1) and its corresponding parameter variables as well as their generated numerical data are presented in tables 1 and 2 below:

Table 1: Description of state spac- with values – model (1)

Variables	Dependent variables Description	Initial values	Units
S_p	Susceptible population to COVID-19 virus	0.0	
X_p	Exposed population	0.0	
A_u	Unaware asymptotic infectious population	0.0	
I_a	Aware infective population	0.0	
I_s	Isolated infectious population	0.0	
S_s	Super-spreaders infectious population	0.0	
H_i	Hospitalized infectious population	0.0	$cells/ml^3$
R_p	COVID-19 recovered population	0.0	
C_v	Aerosol infectious virions	0.025	$copies/ml$
E_I	Immune effectors	0.1	

Note: Tables 1is an inclusive modified data from models [4,17]

Table 2: Description of constants and parameter values for model (1)

Parameter symbols	Parameters and constants Description	Initial values	Units
b_p	Source rate of susceptible population	$b_p \le 10.5$	ml^3d^{-1}
μ	Natural death rate for all sub-population	0.1	day^{-1}
k	Clearance rate of virus	0.25	
$\alpha_{i(i=1,..,5)}$	Death rates due infection at varying stages	0.2;0.3;0.0;0.4; 0.5	
$\tau_{i=1,2}$	Rate at which I_a progresses to I_s and S_s	0.3, 0.5	
$c_{i(i=1,..,5)}$	Rates of contact of susceptible with various infectious stages	0.5;0.4;0.3;0.2; 0.1	
$\eta_{i=1,2,3}$	Rates of recovery from H_i, I_s and S_s	0.5; 0.27;0.13	
$\beta_{i(1,..,5)}$	Probability of interactions of susceptible with varying infectious classes	0.32;0.27;0.175; 0.125;0.05	$ml^3vir^{-1}d^{-1}$

$\varphi_{i=1,2}$	Proportions of A_u that progresses to H_i and S_s	0.3;0.18	
λ	Proportion of X_p becoming A_u	0.58	
θ	Proportion of A_u becoming I_a	0.32	
$\sigma_{i=1,2,3}$	Proliferation of recovered population to susceptible	0.14;0.6, 0.24	
γ_s	Proportion of S_s progressing to I_s	0.22	
δ_h	Proportion of I_s progressing to H_i	0.14	
$\rho_{i=1,2}$	Proportion of I_a progressingto I_s and H_i	0.34; 0.48	
$(1-\rho_1-\rho_2)$	Proportion of I_a that progresses to S_s	0.18	ml^3d^-
$u_{i(i=1,2)}(t)$	Rates at whichface-masking and social distancing are used	$u_i := \begin{Bmatrix} u_i \in [0,1] \setminus 0 \leq \\ (u_1,u_2) < 0.5 \end{Bmatrix}$	
$a_{i(i=1,2)}(t)$	Treatment control functions (HCQ and AZT)	$a_i \in [0,1]$	
$v_{i=1,2}$	Vaccination rates to S_p and I_s compartments	0.06; 0.04	day^{-1}
$m_{i=1,2}$	Immune-induced recovery and clearance rates	1.0×10^{-5}	$ml^3cell^{-3}d^{-1}$
$\omega_{i=1,2}$	Average lifetime of immature viruses	0.01; 0.01	
s	Per-capita rate of aerosol viral load	0.73	day^{-1}
Q	Carry capacity of aerosol viral load	5.0	$cellsml^{-1}$
μ_v	Virions death rate	0.33	day^{-1}
ϕ	Rate of mass action (incidence rate)	0.5	
ζ_E	Source rate for immune effectors	0.8	$cellsml^{-1}d^{-1}$
b_E	Maximum birth rate for immune effectors	0.3	day^{-1}
C_b	Saturation constant for immune effectors birth	100	$cellsml^{-1}$
d_E	Maximum death rate for immune effectors	0.25	day^{-1}
C_d	Saturation constant for immune effectors death	500	$cellsml^{-1}$
μ_E	Natural death rate for immune effectors	0.1	day^{-1}

Note: Tables 1are generated and modified data, [4, 20, 21,22, 23]

3.0 Mathematical Analysis of derived model

In this section, we investigate the mathematical properties that constitute our basic system (1). These include: the boundedness of system solution in certain invariant region denoted by Ω , verification of non-negativity of system solutions and existence and uniqueness of system solutions

3.1 Boundedness of solution

Theorem 1: Let Ω_D denote the entire region understudy, then all solution of model (1) is bounded and: positively invariant in the region

$$\Omega_D = \Omega_N \times \Omega_v, \qquad (3)$$

where

$$\Omega_N = \left\{ (S_p, X_p, A_u, I_a, I_s, S_s, H_i, R_p, E_i) \in \Re_+^9 : 0 \le \left(S_p(t) + X_p(t) + ... + E_i(t) \right) \le \frac{b_p}{\mu} \right\} \qquad (4)$$

and

$$\Omega_v = \left\{ C_v \in \Re_+ : 0 \le C_v(t) \le \frac{\varepsilon b_p}{\mu_v \mu} \right\}, \qquad (5)$$

for all $\varepsilon = s\left(1 - \frac{C_v}{Q}\right) C_v + (1-\rho_1-\rho_2)\varphi_2 e^{-\omega_2 \alpha_1} S_s + [(1-a_1)(1-a_2)[\varphi_1 + \rho_2 + \delta_h]] e^{-\omega_2 \alpha_1} H_i$.

Proof Invoking existing results for boundedness of solutions, [4, 20, 34], we begin by diffusing basic model (1) into human $N(t)$ and virus populations $C_v(t)$. Then, taking the sum of the derivative for $N(t)$ from the model (1), we have

$$\frac{dN}{dt} = b_p - \mu N - \hat{\alpha}\hat{N} + \zeta_E - \mu_v E_i$$

If population is free of virus, then death rates due to infection at varying stages denoted by $\hat{\alpha}_{i(i=1,,,5)} = 0$. That is, we have

$$\frac{dN}{dt} = b_p - \mu N + \zeta_E - \mu_v E_i$$

or

$$\frac{dN}{dt} + \mu N \le b_p + \zeta_E - \mu_v E_i.$$

Integrating in the presence of initial conditions, we obtain

$$N(t) \le \frac{(b_p + \zeta_E)}{\mu} + \left(N(0) - \frac{(b_p + \zeta_E)}{\mu} \right) e^{-\mu t}.$$

Thus, taking limit as $t \to \infty$, we have

$$\underset{t\to\infty}{Lim} \quad N(t) \le \frac{(b_p + \zeta_E)}{\mu}. \qquad (6)$$

Similarly,

$$\frac{dC_V}{dt} = \varepsilon(S_s + H_i) - \mu_v C_v \le \varepsilon \frac{b_p}{\mu} - \mu_v C_v,$$

or

$$\underset{t\to\infty}{Lim} \quad N(t) \le \frac{\varepsilon b_p}{\mu_v \mu}. \qquad (7)$$

From Eqs (6) and (7), we see that the human and virus populations are biologically feasible in the regions (4) and (5), which is defined by Eq. (3) i.e.

$\Omega_D = \Omega_N \times \Omega_v \subset \Re_+^9 \times \Re_+$.

This imply that solution of model (1) with initial conditions is bounded in the invariant region (3) for all $t \in [0,\infty)$ .therefore, the system is well posed.

□

3.2 Non-negativity of model solutions

We use the following theorem to show that the system solutions remain positive for all $t \geq 0$.

Theorem 2: Let $\{S_p(0), X_p(0), A_u(0), I_a(0), I_s(0), S_s(0), H_i(0), R_p(0), C_v(0), E_i(0) \geq 0\} \in \Re_+^{10}$ be the initial conations of system (1). Then, the solution set $\{S_p(t), X_p(t), A_u(t), I_a(t), I_s(t), S_s(t), H_i(t), R_p(t), C_v(t), E_i(t)\}$ of system (1) is non-negative for all $t \geq 0$.

Proof: We invoke existing results of positivity, [21,25]. Then, taking on the equation of system (1), we deduce that for all $t > 0$,

$$\frac{dS_p}{dt} = b_p + m_1 E_i \sigma_1 X_p + \sigma_2 R_p - \beta_i(\hat{N}) S_p - (\mu + v_1) S_p,$$

where fromEq. (2),

$$\beta_i(\hat{N}) = (1 - u_1 - u_2)\left[\frac{\phi C_v}{Q + C_V}\left(\sum_{i=1}^{5} \beta_i c_i(\hat{N}_i)\right)\right], i = 1,....,5 .$$

That is,

$$\frac{dS_p}{dt} = b_p + m_1 E_i \sigma_1 X_p + \sigma_2 R_p - (1 - u_1 - u_2)\left[\frac{\phi C_v}{Q + C_V}\left(\sum_{i=1}^{5} \beta_i c_i(\hat{N}_i)\right)\right] S_p - (\mu + v_1) S_p$$

Differentiating, we have

$$\frac{dS_p}{dt} \leq b_p - \left\{(1 - u_1 - u_2)\left[\frac{\phi C_v}{Q + C_V}\left(\sum_{i=1}^{5} \beta_i c_i(\hat{N}_i)\right)\right] + (\mu + v_1)\right\} S_p . \qquad (8)$$

Then, at zero mortality rate, Eq. (8) becomes

$$\frac{dS_p}{dt} \leq b_p - (\mu + v_1) S_p ,$$

or

$$\frac{dS_p}{dt} + (\mu + v_1) S_p \leq b_p . \qquad (9)$$

This is a first order homogeneous differential inequality. Applying the integrating factor $IF = e^{\int (\mu + v_1) dt} = e^{(\mu + v_1)t}$, we have

$$e^{(\mu + v_1)t} \frac{dS_p}{dt} + (\mu + v_1) S_p e^{(\mu + v_1)t} \leq b_p e^{(\mu + v_1)t},$$

or

$$\frac{d}{dt}\left[(\mu + v_1) S_p e^{(\mu + v_1)t}\right] \leq b_p e^{(\mu + v_1)t} .$$

Integrating, we have

$$S_p(t)e^{(\mu+v_1)t} \le \frac{b_p}{(\mu+v_1)}e^{(\mu+v_1)t} + A,$$

where A, is the constant of integration. Now, simplifying, we have

$$S_p(t) \le \frac{b_p}{(\mu+v_1)} + Ae^{-(\mu+v_1)t}.$$

Solving for A and taking initial condition for $t=0$, and then by substituting the resulting value, we have

$$S_p(t) \le \frac{b_p}{(\mu+v_1)} + \left(S_p(0) - \frac{b_p}{(\mu+v_1)}\right)e^{-(\mu+v_1)t},$$

or

$$S_p(t) \le S_p(0)e^{-(\mu+v_1)t} + \frac{b_p}{(\mu+v_1)}\left(1-e^{-(\mu+v_1)t}\right), \qquad (10)$$

where $S_{p(0)}$ represent the susceptible population for all $t=0$. Also, we note that for $t \to 0$, $S_p(t) \le S_p(0)$, and for $t \to \infty$, $S_p(t) \le \frac{b_p}{\mu+v_1}$, which implies that $0 \le S_p(t) \le \frac{b_p}{\mu+v_1}$ for all $0 \le t \le \infty$. Furthermore, taking on the entire system (1), then from Theorem 1, we have by recursive argument

$$N(t) \le N(0)e^{-\mu t} + \frac{(b_p+\zeta_E)}{\mu}\left(1-e^{-\mu t}\right), \qquad (11)$$

$$C_v(t) \le C_v(0)e^{-\mu t} + \frac{\Delta b_p}{\mu_v \mu}\left(1-e^{-\mu t}\right), \qquad (12)$$

since, $\Omega_N = N(t)$, $\Omega_C = C_v(t)$ and

$\Delta = s\left(1-\frac{C_v}{Q}\right)C_v + (1-\rho_1-\rho_2)\varphi_2 e^{-\omega_2\alpha_1}S_s + [(1-a_1)(1-a_2)[\varphi_1+\rho_2+\delta_h]]e^{-\omega_2\alpha_1}H_i$. Therefore, taking queue from [26],we observe that all solutions of system (1) is such that the set $\left\{\left(S_p(0), X_p(0), A_u(0), I_a(0), I_s(0), S_s(0), H_i(0), R_p(0), C_v(0), E_i(0)\right) \ge 0\right\} \in \Re_+^{10}$ is autonomous for all $t \ge 0$. Hence, the proof is completed.

□

Remark 1: We shall numerically illustrate the system positivity by simulating Eqs. (10), (11) and (12) in our next section.

3.3 Existence and uniqueness of system solution

Suppose $\Pi : \Re \to \Re_+^{10}$ such that

$$t \mapsto \begin{pmatrix} S_p(t), & X_p(t), & A_u(t), & I_a(t), & I_s(t), \\ S_s(t), & H_i(t), & R_p(t), & C_v(t), & E_i(t) \end{pmatrix}$$

and

$F : \Re \to \Re_+^{10}$ such that

$$\Pi(t) \mapsto F\left(\Pi(t)\right) = \begin{pmatrix} S_p'(t), & X_p'(t), & A_u'(t), & I_a'(t), & I_s'(t), \\ S_s'(t), & H_i'(t), & R_p'(t), & C_v'(t), & E_i'(t) \end{pmatrix}.$$

Then, system (1) becomes

$\Pi(t) \mapsto F\left(\Pi(t)\right)$, $\Pi(0) = \Pi_0$.

Theorem 3: (Existence and Uniqueness of solutions)
System (1) is continuous and satisfies Cauchy-Lipschitz condition.

Proof: Here, invoking results from proofs of existence and uniqueness theorem, [20], we show for one equation and the rest follows same procedure. Let

$$G(t,s) = \frac{dS_p}{dt} = b_p + m_1 E_i \sigma_1 X_p + \sigma_2 R_p - (1-u_1-u_2)\left[\frac{\phi C_v}{Q+C_V}\left(\sum_{i=1}^{5}\beta_i c_i(\hat{N}_i)\right)\right]S_p - (\mu+v_1)S_p \ . \qquad (13)$$

Then, the partial derive with respect to the susceptible population S_p gives

$$\frac{\partial G(t,s)}{\partial S} = -(1-u_1-u_2)\left[\frac{\phi C_v}{Q+C_V}\left(\sum_{i=1}^{5}\beta_i c_i(\hat{N}_i)\right)\right] - (\mu+v_1) \ . \qquad (14)$$

We note that the function $G(t,s)$ and the corresponding partial derive $\frac{\partial G(t,s)}{\partial S}$ is defined and continuous at all point (t,s) . Similarly, the right-hand functions of other equations and their corresponding partial derivatives satisfy these conditions. Hence, from the existence and uniqueness theorem, there exists unique solution for $S_p(t), X_p(t), A_u(t), I_a(t), I_s(t),\ S_s(t), H_i(t), R_p(t), C_v(t)$ and $E_i(t)$ in some open intervals centered at t_0. Next, show that the solution satisfies the Lipschitz condition. That is, using Eq. (13), we observe that

$$\left|G(t,S_{p(1)}) - G(t,S_{p(2)})\right| = \left| \begin{array}{l} \left(b_p + m_1 E_i \sigma_1 X_p + \sigma_2 R_p - (1-u_1-u_2)\left[\frac{\phi C_v}{Q+C_V}\left(\sum_{i=1}^{5}\beta_i c_i(\hat{N}_i)\right)\right]S_{p(1)} - (\mu+v_1)S_{p(1)}\right) \\ -\left(b_p + m_1 E_i \sigma_1 X_p + \sigma_2 R_p - (1-u_1-u_2)\left[\frac{\phi C_v}{Q+C_V}\left(\sum_{i=1}^{5}\beta_i c_i(\hat{N}_i)\right)\right]S_{p(2)} - (\mu+v_1)S_{p(2)}\right) \end{array} \right|$$

$$= \left|(-)\left((1-u_1-u_2)\left[\frac{\phi C_v}{Q+C_V}\left(\sum_{i=1}^{5}\beta_i c_i(\hat{N}_i)\right)\right] + (\mu+v_1)\right)\left(S_{p(1)} - S_{p(2)}\right)\right|$$

$$\leq \left((1-u_1-u_2)\left[\frac{\phi C_v}{Q+C_V}\left(\sum_{i=1}^{5}\beta_i c_i(\hat{N}_i)\right)\right] + (\mu+v_1)\right)\left|S_{p(1)} - S_{p(2)}\right| .$$

This implies that

$\left|G(t,S_{p(1)}) - G(t,S_{p(2)})\right| \leq M\left|S_{p(1)} - S_{p(2)}\right|$,

where, $M = \left((1-u_1-u_2)\left[\frac{\phi C_v}{Q+C_V}\left(\sum_{i=1}^{5}\beta_i c_i(\hat{N}_i)\right)\right] + (\mu+v_1)\right)$ depicts Lipschitz constant with $u_i := \{u_i \in [0,1] \setminus 0 \leq (u_1,u_2) < 0.5\}$. In a similar procedure, we show for the remaining variables satisfying the Cauchy- Lipschitz condition. Thus, there exists a unique

solution $S_p(t), X_p(t), A_u(t), I_a(t), I_s(t), \ S_s(t), H_i(t), R_p(t), C_v(t), E_i(t)$ for all $t \geq 0$.

4.0 Numerical simulations and analysis

Having determined the system proposed model and its corresponding theoretical predictions, we shall present here, the numerical illustrations for system positivity deploying some key state-space. Of note, the simulations shall explore in-built rkfixed Runge-Kutta of order of precision 4 in a Mathcad software. Tables 1and 2provides hypothetically generated data in relation to verified data, [4, 20, 21,22, 23].

4.1 Simulations of system positivity

Here, we numerically illustrate system positivity by simulating Eqs (10)– (12), noting that control functions denoted by $c_{i(i=1,2)}$ is zero, where. $c_i = (u_i, a_i, m_i, \nu_i) = 0$. Thus, invoking program algorithm and its result as depicted by Appendices A1 and A2, we simulate as depicted by the graphical images ofFigs 2–4 below:

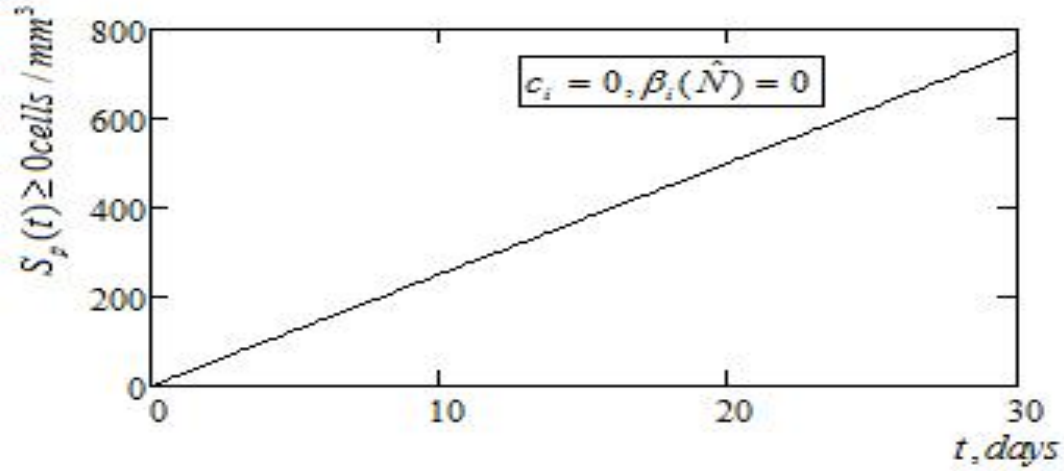

Fig. 2: Graphical image for non-negative COVID-19 susceptible popn,, $t \geq 0$

From Fig. 2, we observe that under zero mortality rate, the susceptible population exhibit smooth incline linear curve with value range of $0 \leq S_p(t) \leq 750.52 cells / mm^3$ for all $t_f \leq 30$ days.

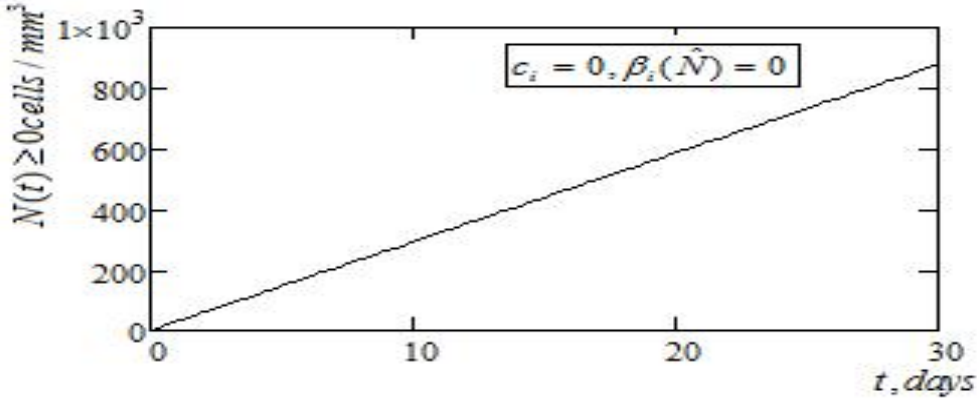

Fig. 3: Graphical image for non-negative COVID-19of varying human popn., $t \geq 0$

Sustaining zero mortality rate, Fig. 3, represent the simulation of the entire human population $N(t)$. We observe that the varying human population exhibit smooth incline linear curve with values varying the range $0 \leq N(t) \leq 878.636 cells/mm^3$ for all $t_f \leq 30$ days.

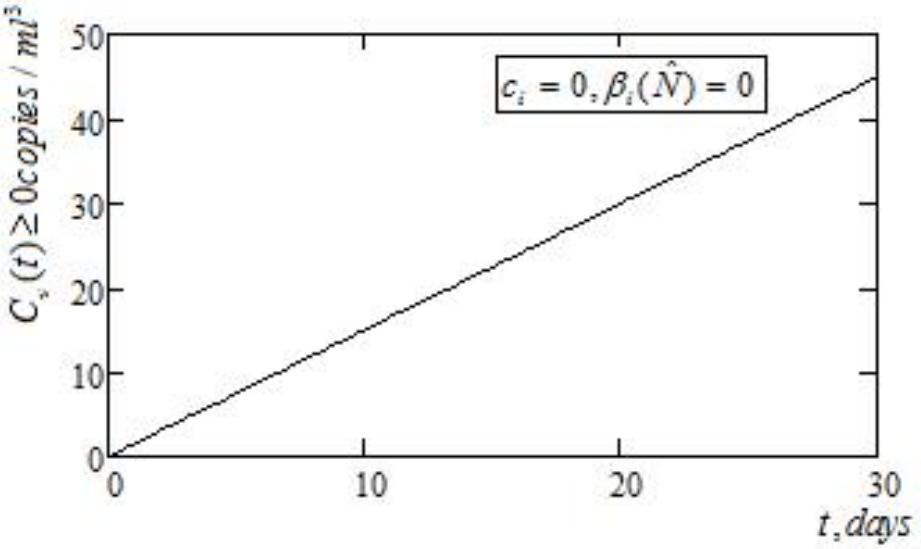

Fig. 4: Graphical image for non-negative COVID-19of varying human popn., $t \geq 0$

In Fig. 4, we simulate the concentrated aerosol viral load. Observe is asmooth incline linear curve representing positive COVID-19 state-space with value in the range of $0.025 \leq C_v(t) \leq 44.925 copies/ml^3$ for all $t_f \leq 30$ days. Clearly, Figs 2-4 indicates that the proposed model exhibit system boundedness, non-negativity and existence and uniqueness of system solutions exist as predicted in theorems 1-3.

5.0 Conclusion

Triggered by the conceptual complex nature of formulating an expanded 10-Dimensional deterministic COVID-19 model that is capable of accounting for the mathematical and epidemiological application of triple-bilinear control functions under combined hypo-hyper transmission modes, the present study had tinkered towards establishing the anticipated model. More importantly, to verified that the model exhibited non-negative and the well-posedness of the system solutions. Proposed model was formulated and system well-posedness investigated theoretically using fundamental theory of differential equations with the incorporation of Cauchy-Lipschitz condition. Furthermore, numerical illustrations were computed and results obtained. The results indicated that proposed model does not only exhibit non-negativity of system state-space but is sufficiently bounded and well-posed. Therefore, the present model exhibit sufficiency for the investigation of system mathematical and epidemiological well-posed within the dynamical invariant region $\Omega_D = \Omega_N + \Omega_C \in \Re_+^9 \times \Re_+$.

6.0 Data availability

The authors declared that all data and parameter values used for the simulations of this mathematical model has been cited accordingly.

Funding and acknowledgment

This research, which is the Phase-I of the two required publications is under a grant funded by TETFund-IBR in conjunction with University of Cross River State, Calabar, within project no. **TETF/DR&D/UNI/CAL/RG/2021/Vol.1**. Our utmost thanks to TETFund for their generosity.

Declaration of competing interest

The authors declared that there exists no conflict of interest and the work done is an original research that has not been tendered for consideration.

Credit authorship contribution statement

Bassey Echeng Bassey: Conceptualization, methodology, writing – draft, reviews and editing, software programing, analysis and writing final reversion. **Igwe O. Ewona**: Methodology, spear-headed grant, supervision, formal analysis, editing and validation.

References

[1] Torres D. F. M., Ndaïrou F., Area I. and Nieto J. J. (2020) Mathematical modeling of COVID-19 transmission dynamics with a case study of Wuhan. Chaos, Solitons and Fractals. Retrieved date: [02, June, 2022], online available athttp://ees.elsevier.com

[2] Gumel A. B. (2020) Using mathematics to understand and control the coronavirus pandemic. Retrieved date: [15, May, 2022], online available at https://opinion.premiumtimesng.com /2020/05/04/using-mathematics-tounderstand-and-control-the-coronavirus-pandemic-by-abba-b-gumel/.

[3] Salehi S, Abedi A., BalakrishnanS.andGholamrezanezhad A. (2020) Coronavirus disease 2019 (COVID-19): a systematic review of imaging findings in 919 patients. Am J Roentgenol (2020):1–7.

[4] Bassey E. B. and Atsu U. J. (2021) Global stability analysis of the role of multi-therapies and non-pharmaceutical treatment protocols for COVID-19 pandemic. Chaos, Solitons and Fractals, 143 (2021) 110574 https://pubmed.ncbi.nlm.nih.gov/33519116/ or at: https://www.sciencedirect.com/science/article/abs/pii/S0960077920309656?via%3Dihub

[5] Leslie M. (2020) T cells found in coronavirus patients 'bode well' for long-term immunity. Retrieved date: [14, December, 2021], online available athttp://science.sciencemag.org/content/368/6493/809

[6] Grigorieva E., Khailov E. and Korobeinikov A. (2020) Optimal quarantine strategies for COVID-19

control models. Retrieved date: [29, January, 2022], online available at https://arxiv.org/pdf/2004.10614.pdf

[7] Li Q., Wu P., et al. (2020) Early Transmission Dynamics in Wuhan, China, of Novel Coronavirus–Infected Pneumonia. The new england journal of medicine, 382 (13): 1199-1207. https://www.nejm.org/doi/pdf/10.1056/NEJMoa2001316?articleTools=true

[8] Bekker L. and Mizrahi V. (2020) COVID-19 research in Africa. Retrieved date: [29, April, 2022], online available at: http://science.sciencemag.org/content/368/6494/919

[9] Asamoah J. K. K., Owusu M. A., Jin Z., Oduro F. T., AbidemiA.and Gyasi E. O. (2020) Global stability and cost-effectiveness analysis of COVID-19 considering the impact of the environment:using data from ghana. Chaos Solitons Fractals, 140:110103. http://dx.doi.org/10.1016/j.chaos.2020.110103.

[10] Bassey E. B. (2022) Impact of Optimal Control Techniques on Dual-Bilinear Treatment Protocols for COVID-19 Pandemic. Journal of Applied Mathematics and Computation, 6(3): 310-331. DOI: 10.26855/jamc.2022.09.004 https://www.hillpublisher.com/journals/JAMC/

[11] Chen T-M., Rui J., Wang Q-P., Zhao Z-Y., Cui J-A.and Yin L. (2020) A mathematical model for simulating the phase-based transmissibility of a novel coronavirus. Infect Dis Poverty, 9:1–8.

[12] Wan H., Cui.J-a and Yang G-J. (2020) Risk estimation and prediction by modeling the transmission of the novel coronavirus (COVID-19) in mainland China excluding Hubei province. Infect Dis Poverty, 9(1):1-16. doi: 10.1186/s40249-020-00683-6.https://pubmed.ncbi.nlm.nih.gov/32831142/

[13] Jahanshhi H., YousefpourA.andBekires S. (2020) Optimal policies for control of the novel coronavirus disease (COVID-19) outbreak. Chaos, Solitons and Fractals, 136:1-6. https://www.ncbi.nlm.nih.gov/pmc/articles/PMC7229919/

[14] Wu J. T., Leung K. and Leung G. M. Nowcasting and forecasting the potential domestic and international spread of the 2019.nCoV outbreak originating in Wuhan, China: a modeling study. The Lacet 2020; **395**(10225):689-697. https://www.thelancet.com/action/showPdf?pii=S0140-6736%2820%2930260-9

[15] Obsu L. L. and Balcha F.S. (2020) Optimal control strategies for the transmission risk of COVID-19. Journal of Biological Dynamics, 14(1):590-607. https://www.tandfonline.com/doi/full/10.1080/17513758.2020.1788182

[16] Suyanto S., Sasmita N. R., Ikhwan M. and Chongsuvivatwong V. (2020) Optimal control on a mathematical model to pattern the progression of coronavirus disease 2019 (COVID-19) in Indonesia. Global Health Research and Policy 2020; 5(38): 1-12. https://ghrp.biomedcentral.com/articles/10.1186/s41256-020-00163-2

[17] Altan A. and Karasu S. (2020) Recognition of COVID-19 disease from X-ray images by hybrid model consisting of 2D curvelet transform, chaotic salp swarm algorithm and deep learning technique. Chaos, Solitons and Fractals, 140 (2020) 110071, 1-10.

[18] Nana-Kyere S., Boateng F. A., Jonathan P., Donkor A., Hoggar G. K ., Desmond Titus B. D. , Kwarteng D. and Adu K. I. (2022) Global Analysis and Optimal Control Model of COVID-19. Computational and Mathematical Methods in Medicine, (2022), 1-20. Article ID 9491847, 20 pages https://doi.org/10.1155/2022/9491847

[19] Cacciapaglia G., Corentin Cot C. and Sannino F. (2020) Second wave COVID- 19 pandemics in Europe: a temporal playbook. Scientifc Reports, 10:15514 | https://doi.org/10.1038/s41598-020-72611-5

[20] Ezegu N. J, Togbenon H. A. and Moyo E. (2019) Modeling and analysis of cholera dynamics with vaccination. Am J Appl Math Stat, 7(1):1–8, https://www.academia.edu/38126262/Modeling _ and _ Analysis _ of _ Cholera _ Dynamics _ with _ Vaccination

[21] Edward S, Nyerere N. (2015)A mathematical model for the dynamics of cholera with control measures. ApplComput Math, 4(2):53–63. http://www.sciencepublishinggroup.com/journal/paperinfo?journalid=147&doi=10.11648/j.acm.20150402.14

[22] Hattaf K. and Yousfi N. (2018) Modeling the adaptive immunity and both modes of transmission in HIV infection. Computation, 6(37): 1-18.

[23] Adams B. M., Banks H. T., Hee-Dae K. and Tran H. T. (2004) Dynamic Multidrug Therapies for HIV: Optimal and STI Control Approaches. Retrieved date: [24, July, 2022], online available at http://citeseerx.ist.psu.edu/viewdoc/summary?doi=10.1.1.400.9056

[24] Osman S, Makinde O. D, Theuri D. M. Stability analysis and modeling of listeriosis dynamics in human and animal population. Glob J Pure Appl Math 2018;14(1):115–38.

https://www.ripublication.com/gjpam18/gjpamv14n1 _ 08. pdf .

[25] Mtisi E., Rwezaura H. and Tchuenche J. M. (2009) A mathematical analysis of malaria and tuberculosis co-dynamics. Discrete ContDynSyst B,12(4):827–64.

[26] Ringa N.,Diagne M. L., Rwezaura H., OmameA., Tchoumi S. Y. and

Tchuenche, J. M. (2022) HIV and COVID-19 co-infection: A mathematical model and optimal control. Informatics in Medicine Unlocked, 31 (2022) 100978. http://www.elsevier.com/locate/imu

APPENDIX A – Figures 2-4

A1. Program Algorithm for positivity of COVID19 model

$N0 := 0.0 \qquad C0 := 0.0 \qquad Ss := 0.0 \qquad Hi := 0.0$

$Sp := 0.0$

$z := 3$

$H := (0.0 \quad 0.0 \quad 0.0)^T$

$$F(t, H) := \begin{bmatrix} D \leftarrow s \cdot \left(1 - \frac{Cv}{Q}\right) \cdot Cv + [(1 - \rho 1 - \rho 2) \cdot \varphi 2] \cdot e^{-\omega 2 \cdot \alpha 1} \cdot Ss + [(1 - a1) \cdot (1 - a2) \cdot (\varphi 1 + \rho 2 + \delta h)] \cdot e^{-\omega 2 \cdot \alpha 1} \cdot Hi \\ F_1 \leftarrow Sp \cdot e^{-(\mu + \nu 1) \cdot z} + \frac{bp}{(\mu + \nu 1)} \cdot \left[1 - e^{-(\mu + \nu 1) \cdot z}\right] \\ F_2 \leftarrow N0 \cdot e^{-(\mu \cdot z)} + \left(\frac{bp + \zeta E}{\mu}\right) \cdot \left[1 - e^{-(\mu \cdot z)}\right] \\ F_3 \leftarrow C0 \cdot e^{-(\mu \cdot z)} + \frac{D \cdot bp}{\mu \cdot \mu v} \cdot \left[1 - e^{-(\mu \cdot z)}\right] \\ F \end{bmatrix}$$

A2. Result from simulations

$J := \text{rkfixed}(H, 0, T, n, F) =$

	1	2	3	4
1	0	0	0	0
2	0.3	7.505	8.786	0.449
3	0.6	15.01	17.573	0.898
4	0.9	22.516	26.359	1.348
5	1.2	30.021	35.145	1.797
6	1.5	37.526	43.931	2.246
7	1.8	45.031	52.718	2.695
8	2.1	52.536	61.504	3.145
9	2.4	60.042	70.29	3.594
10	2.7	67.547	79.076	4.043
11	3	75.052	87.863	4.492
12	3.3	82.557	96.649	4.942
13	3.6	90.062	105.435	5.391
14	3.9	97.568	114.221	5.84
15	4.2	105.073	123.008	6.289
16	4.5	112.578	131.794	...